Journal of Computational Applied Mechanics 2022, 53(3): 309-331

DOI: 10.22059/jcamech.2022.342953.721

RESEARCH PAPER

Exact analytic solution for static bending of 3-D plate under transverse loading

Festus Chukwudi Onyeka [a], Thompson Edozie Okeke [b], Chidobere David Nwa-David [c], Benjamin Okwudili Mama [b,*]

[a] *Department of Civil Engineering, Edo State University Uzairue, Edo State, 312102, Nigeria.*
[b] *Department of Civil Engineering, University of Nigeria, Nsukka, Enugu State, 410101, Nigeria.*
[c] *Department of Civil Engineering, Michael Okpara University of Agriculture, Umudike, Abia State, 440109, Nigeria*

Abstract

In this study, an exact solution for the bending analysis of a three-dimensional (3-D) rectangular plate under transverse loading is presented using the fundamentals of elasticity theory. The theoretical model whose formulation is based on static elastic principle considered transverse shear deformation and still obviates the need for the shear correction factor effect which is associated with refined plate theory (RPT). As an improvement to RPT, the equations of equilibrium are obtained from elastic principle using 3-D kinematic and constitutive relations which is later converted to energy equation using general variation to get the deflection and rotation relationship. The solution of the equilibrium equation produced an exact trigonometric displacement function which is a product of the plate's coefficient of deflection and shape function. By minimizing the general energy equation with respect to the coefficients of deflection and shear deformation rotation, a theoretical model for calculating the deflection, moment and stresses of thick rectangular plate were obtained. The result shows that, at a span - depth ratio between 4 and 30, deflection values vary between 0.0063 and 0.0054. At the span - depth ratio 30 and above, a constant value of 0.0054 is noticed, this value is equal to the value of the CPT. The value of transverse shear stress along y-z coordinates varies between 0.00198 and -0.0001. The value of transverse shear stress along y-z coordinates being less than or equal the value showed that this value is the same as that of CPT. It can be deduced that at a span - depth ratio between 4 and 30 the plate is regarded as thick. The plate's span - thickness ratio of 30 and beyond is regarded as thin or moderately thick because its value at this point coincides with the value of the CPT. The comparative analysis between the present results and other theories shows that this 3-D predicts the vertical displacement, moments and the stresses more accurately than previous studies considered in this paper. It was observed that the present theory varied more with those of those of 2-D numeric analysis and 2-D HSDT with about 7.83% and 6.01%. Meanwhile, the recorded percentage differences showed that a derived 2-D HSDT predicted accurately the bending characteristics of the plate with 2.55%, proving that assumed deflection is coarser for the thick

* Corresponding author. Tel.: +23 8068285789; ORCID: https://orcid.org/0000-0002-2668-9753
E-mail address: boniface.mama@unn.edu.ng or onyeka.festus@edouniversity.edu.ng

plate analysis. It is concluded that, unlike an assumed function, a derived 2-D theory can give a close form solution, but a typical 3-D theory of elasticity is required for an exact solution of a rectangular plate and can be recommended for the analysis of any type of rectangular plate with such loading and boundary condition.

Keywords: Exact static theory; equilibrium equation; bending of 3-D clamped plate; trigonometric model

1. Introduction

Plates are structural elements that are three-dimensional, and whose thickness is little compared with the other plane and parallel surfaces [1]. Plates have vast applications in structural, aeronautical, mechanical, naval, and Geotechnical engineering for the modeling of retaining walls, ship hulls, roof, and floor slabs, and foundation slabs [2, 3].

As regards geometry, plates can be classified as elliptical, skew, circular, rhombic, square or rectangular. Based on the properties of the material, plates are defined as heterogeneous, homogeneous, orthotropic, anisotropic or isotropic [4]. Generally, plates can have simply supported, clamped, or free edge conditions. Based on the ratios of the thickness (t) to the least lateral dimension (a), plates are classified as thin plates, moderately thick plates and thick plates [5, 6]. Rectangular plates with $50 \leq a/t \leq 100$ have been defined as thin plate, $20 \leq a/t \leq 50$ as moderately thick and $a/t \leq 20$ as thick plate where a/t is the span-to-depth ratio, according to [7]. The pertinence and captivating attributes of thick plates in engineering structures have increased its research interest among scholars. In engineering, thick plates are mostly preferred due to its exceptional features such as; light weight, heavy loads carrying capacities, reduction in cost, and high mechanical properties [8]. This study considers isotropic rectangular thick plate for its bending analysis.

Research areas of thick plate analysis include vibration, buckling and bending [9]. Bending occurs when the plate deforms at right angles towards the surface of the plate [10] and this occurrence is a result of induced forces and impact of moments. The plate begins to fail when the lateral deflection increases as the applied load exceeds the critical load [11]. This critical load value which determines the stability of the plate, should be calculated in order to properly analyze the plate. Basically, structural breakdown may result from deformations when not examined thoroughly. Investigating the bending mannerism of thick plates is therefore necessary so as to make sure that the plates are safe for load resistance.

To depict the bending attribute of thick plates, several theories have been formulated, developed and employed. The theories include; CPT, also referred to as Kirchhoff plate theory [12], and refined plate theories (RPT) such as; FSDT, TSDT [12], ESDT [13], PSDT [14] and the HSDT [15]. CPT does not account for transverse shear effects; hence it cannot determine the exact bending behavior of thick plates. To overcome the limitations of CPT, FSDT was introduced but the correction factor was needed [16, 17] for it to give the desired outcome.

HSDT was created as an amelioration to surmount the shortcomings of CPT and FSDTs. These HSDTs consider the deformation effects without the use of correction factors [18, 19] and provides accurate solutions in predicting the bending behavior of thick isotropic plates. These RPTs are regarded as 2-D theories as it neglects the normal strain and stress along the thickness axis of the plate. Since plates are three-dimensional structural elements, a typical 3-D theory ought to be employed to ensure exact bending solutions and this validates the usefulness of this study.

Various methods such as the analytical methods (closed-form approach) and numerical methods (approximate approach) [20], can be used to analyze the bending characteristics of thick plates. Analytical methods are mathematical techniques that solve plate problems, satisfying the governing equations on the boundaries of the plate and in all the points on the plate surface. They include: Levy series, Navier series, Eigen expansion methods, as well as the method of integral transforms [21]. Analytical method has been used by several authors such as [22-24] to solve plate bending problems for different support conditions and different loading conditions.

Where the bending problem seems complicated and closed form solutions are difficult to obtain, numerical methods are employed to obtain approximate results. Numerical methods consist of weighted residual, finite element, boundary element, finite difference, Bubnov-Galerkin, Variational Galerkin, Variational Ritz, Collocation and Variational Kantorovich methods. Several researchers such as [25-27] have widely used numerical methods to analyze different plate problems.

Energy2 methods can be numerical or analytical. The total energy is same as the addition of all the strain energy and potential energy or external work on the continuum [28]. This method consists of Ritz, minimum potential energy, Raleigh-Ritz and Galerkin. An analytical method with the energy approach will be considered in this study since it yields exact solutions.

2. Literature Review

Ike [29] used the Fourier series method with hyperbolic shear deformation theory to satisfactorily obtain the bending solutions of thick beams. Avoiding the shear correction factors of FSDTs, the author was able to achieve transverse shear stress free conditions at the top and bottom surfaces of the beam using hyperbolic sine and cosine functions. The author failed to apply 3-D plate theory and CSCS boundary condition was not considered.

Variational method to polynomial shape function were applied by Ibearugbulem *et al.* [30] to determine the displacements and stresses of the CCCC rectangular thick plate. No correction factor was applied to satisfy the zero shear-stress state at the plate surfaces. The authors failed to incorporate 3-D theory in their analysis. The use of trigonometric energy potential function was not considered. They also failed to address CSCS plates.

Applying a polynomial displacement function with a modified deformation theory, Onyeka *et al.* [31], determined the lateral critical imposed load used to investigate the trait of an isotropic plate in their static bending analysis. The authors failed to employ an energy potential trigonometric function in their study. The authors failed to consider plates with CSCS [C -Clamped; S-Simply Supported] and the deflection as well as the shear deformation along the direction of the z - axis were not obtained.

Sayyad and Ghugal [32] solved the bending issue of SSSS rectangular plates with exponential functions and refined shear deformation theory to obtain the displacements and stresses. They achieved this without the use of correction factor and their result was found satisfactory when compared with other refined theories. They also did not apply 3D theory; neither did they use energy potential function. Their study failed to cover CSCS plates.

Virtual work principle and HSDT were used by Ghugal and Gajbhiye [13], to analyze the bending of simply supported isotropic plate. The authors considered the shear and strain deformation effect without using the shear correction factor associated with FSDTs. The state of the zero shear transverse stresses was satisfactory. Although the authors did not consider applying three-dimensional plate theory, they obtained closed-form results that are very close to exact 3-D solutions because of their analytical approach. The energy function was not used. They did not cover plates with CSCS support conditions.

The Ritz method was employed by Nwoji *et al.* [21] to solve SSSS Kirchhoff plate bending problem. The authors obtained closed-form solutions using the analytical method. However, the theory employed in their study cannot be applied to thick plates to get accurate results. The energy potential function and 3-D theory were not used in their study. The authors failed to cover CSCS plates.

Onyeka & Okeke [33] and Mantari *et al.* [34] obtained the displacement and stresses in thick rectangular plate using shear deformation plate theory. Onyeka and Okeke [33] used 2-D plate theory based on HSDT and applied to get the blending solution on a thick plate using polynomial displacement function, but they did not analyze the stresses along the thickness axis and this made their solution not to be exact. In the same way, Mantari *et al.* [34], employed trigonometric theory for the static bending analysis of a thick plate. However, both [33] and [34] failed to consider plates with the CSCS boundary condition.

Onyeka *et al.* [35] applied RPT and polynomial displacement function to analyze thick plates. The authors evaluated CSCS plates and the in-plane displacements, deflections, moments, shear force, also the deformation rotations at the plates' arbitrary points. The strain and stress along the thickness direction were neglected. Trigonometric function was not considered in their study. The authors employed incomplete 3-D elasticity theory for the three-dimensional equilibrium equations and cannot be reliable for thick plate analysis as they cannot give an exact solution.

Using the numerical approach and the 3-D plate theory, Grigorenko *et al.* [36] analyzed the bending of all-round clamped plates. The authors applied two coordinate directions of spline collocation and the results obtained were satisfactory. They did not employ analytical methods in their work; therefore, could not obtain exact solutions. Their study also failed to address CSCS plates.

Ibearugbulem *et al.* [37], analyzed the bending of thick plates with simply supported edges, obtaining exact polynomial displacement function from the governing equation with an analytical technique. The trigonometric function was not applied. The solutions of polynomial function as used tend to infinity while the application of trigonometric function which is employed in this study, yields closed form solution. Their study was three-dimensional, but they failed to cover plates with CSCS support conditions.

To solve the bending problem of isotropic thick plate with simply supported edges (SSSS), Onyeka and Mama [38] employed trigonometric shape functions with direct vibrational energy technique. Although the authors employed the 3-D plate theory, they failed to use the energy potential functional and plates with CSCS boundary conditions were not addressed.

Three-dimensional elasticity theory was used by Hadi *et al* [39] to investigate the bending of rectangular plate that consists of functionally graded material with the variable exponential properties. Using a numerical example, the authors studied the impact of several functionally-graded variation on the stress and displacement fields. Their study

showed significant effects of graded material properties on the plate's behavior. The authors presented exact solutions of the stresses and displacements. However, the authors failed to consider trigonometric functions which produce a reliably exact solution and CSCS bounded rectangular plates.

Recently, most researchers have employed non-classical elasticity theories to analyze plates [40]. Couple stress theory, nonlocal elasticity theory, surface theory, strain gradient theory and nonlocal strain gradient theory have been used to study nanostructures [41, 42]. Applying consistent couple-stress theory and nonlocal elasticity theory, Nejad *et al* [43-47] have presented studies on elasticity, buckling and vibrations of beams made of functionally graded materials (FGM). The elasticity of FGM structures of variable thickness was also presented by Hosseini *et al* [48, 49]. Mohammadi *et al* [50-82], also presented studies on the elasticity, vibration and buckling behavior of nano structured plates and beams. A 3-D plate theory for bending analysis of rectangular thick plates was not considered. These authors failed to analyze the bending behavior. Their study was not centered on isotropic rectangular plates. neither did they consider the three-dimensional plate theory, not consider CSCS plate boundary condition in their analysis.

Nonlocal strain gradient elasticity theory and Hamilton's principle were employed by Hadi *et al* [83], Hosseni [48], Mohammadi [79], Shishesaz and Hosseni [84], and Shishesaz *et al* [85] to analyze FGMs. Mazarei *et al* [86] used von Mises yield criterion to formulate a plastic model for its analysis. The authors in [83] examined the effects of material constant and small-scale parameters. In [48] and [84], the authors investigated the effect of graded index, higher order stresses and thickness profile on stresses. Couple-stress theory was applied by Hadi *et al* [87], Gorgani *et al* [88], and Barati et al [89] to capture the size effects of FGMs. These scholars failed to analyze isotropic thick plates. The 3-D plate elasticity theory and bending analysis was also not taken into account during their investigations. More so, many scholars have performed different studies using the refined plate theory, but very few studies have been carried out applying 3-D plate theory on the bending of thick plates of different boundary conditions using different methods and techniques. Since plates are three-dimensional elements, analyzing the shear distortion aftermath in the spatial dimensions along x, y and z axes, will eliminate the problem of unreliable design due to 2-D application in the construction industry. This research gap has prompted this present study.

This present study, unlike the previous studies which were gleaned from the displacement functions and refined plate theories and some orthotropic 3-D buckling and vibration analysis, considered the 3-D theory of elasticity with trigonometric function in order to achieve a close form (exact) solution in determination of bending characteristics of plate under CSCS boundary condition. The analytical technique was used to design the methodology via a variation calculus. The advantages of the applied technique are that, it gives exact results, in order to adequately meet the governing equations in the plate domain and across the edges of the plate. The method circumvents the tedious process of solving double Fourier which is associated with exact solution processes using Euler's formulation. Most of the former studies in this regard employed the numerical method to avoid this tedious process, but it is recorded that the numerical method appears limited as it produces approximate solutions [30] and the stresses & displacements at any point in the plate cannot be determined. More so, trigonometric functions produce an exact solution unlike polynomial, exponential and hyperbolic whose exact function tends to infinity [35]. Furthermore, a plate which is a 3-D element is ought to analyse as such to ensure accuracy and structural safety, unlike previous studies which made some comfortable assumptions about the kinematics of deformation and state of state by neglecting the stress along the thickness axis of the plate. Hardly can one see works a typical 3-D bending analysis of thick plates based on based on the variational principle and trigonometric functions. This research gap attracts more attention; hence this research work is needed as the gap is worth filling. Meanwhile the limitation can be seen in this work, as the mathematical complexity exists in the 3-D analysis of plate. In a thorough mathematical way, the governing equations of the bending problem is unravelled using analytical technique to get satisfactory closed form solutions. The focus of this work is to study the exact bending behaviour of a three-dimensional rectangular plate with support conditions of two opposite short edges clamped and simply supported on two opposite long edges (CSCS), subjected to uniform distributed transverse loads. The effect of deflection and the stresses on the plate will be determined.

3. Research Methodology

The research methodology of this study is presented by considering a rectangular plate in the Figure 1 to be deformable in three dimensional (x, y, z) Cartesian coordinates: length (a), width (b) and thickness (t). The theoretical framework is based on the 3-D static elastic theory of plate.

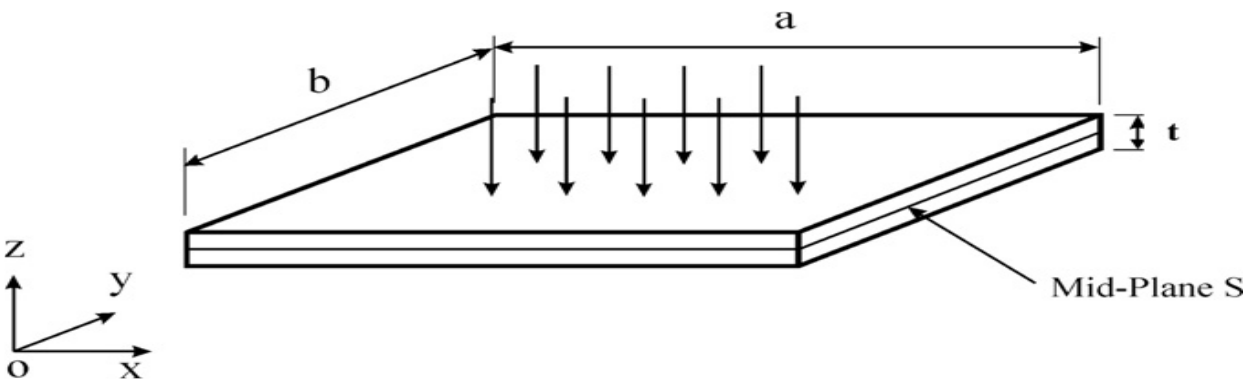

Fig 1: An element of thick rectangular plate showing middle surface

An analytical modelling approach based on energy method was used to obtain formulas for the analysis. The procedures of formulating the potential energy equation in the form of the kinematics and three-dimensional constitutive relations for a static elastic theory of plate, thereafter, the governing equations were derived and solved to obtain formula for the analysis.

3.1. Basic Assumptions

The basic assumptions made in the formulation of the plate theory includes:
(i) The plate material is isotropic, homogenous and linearly elastic.
(ii) The load intensity of the plate is transverse distributed uniform load.
(iii) A flat x-z or y-z section, which is normal to the middle x-y plane before bending shall no longer remain normal to the middle x-y surface after bending.
(iv) The elastic yield stress exists at a considerable small deflection.

3.2. Kinematics

As shown in Figure 2, the spatial dimensions of the plate along x, y and z-axes are a, b and t respectively. The displacement field which includes the displacements along x, y and z-axes: u, v and w are obtained assuming that the x-z section and y-z section, which are initially normal to the x-y plane before bending go off normal to the x-y plane after bending of the plate (see Figure 2).

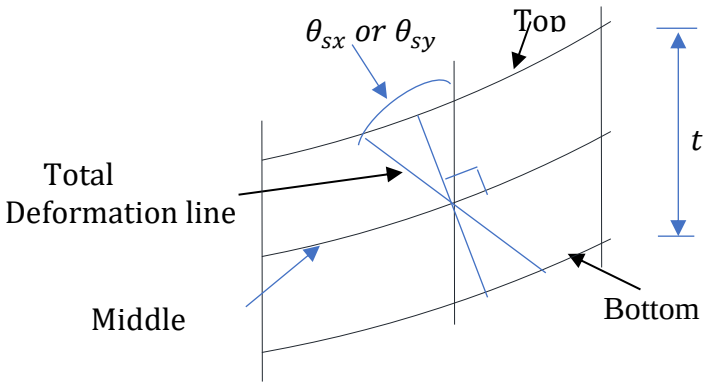

Fig 2: Rotation of x-z (or y-z) section after bending

Considering the assumption of the thick plate as stated in section 3.1, the deformation diagram in Figure 2 can be resolved using trigonometric relations for small angles, the algebraic relationship between the slope along the x axis and y becomes:

$$\theta_{sx} = \frac{\partial u}{\partial z} \tag{1}$$

$$\theta_{sy} = \frac{\partial v}{\partial z} \tag{2}$$

The non-dimensional form of the in-plane displacement along x and y axis can be written as presented in Equation (2) and (3) gives:

$$u = ts.\theta_{sx} \tag{2}$$

$$v = ts.\theta_{sy} \tag{3}$$

Where:

$$z = ts \tag{4}$$

Thus, the three non-dimensional coordinates normal strain components were derived using strain-displacement expression according to Hooke's law and presented in Equation (4) - (7):

$$\varepsilon_x = \frac{1}{\mathrm{a}}.\frac{\partial u}{\partial R} \tag{5}$$

$$\varepsilon_y = \frac{1}{\mathrm{a}\beta}.\frac{\partial v}{\partial Q} \tag{6}$$

$$\varepsilon_z = \frac{1}{\mathrm{t}}.\frac{\partial w}{\partial s} \tag{7}$$

Similarly, the three non-dimensional coordinates shear strain components were derived using strain-displacement expression according to Hooke's law and presented in Equation (8) - (10):

$$\gamma_{xy} = \frac{1}{\mathrm{a}\beta}.\frac{\partial u}{\partial Q} + \frac{1}{\mathrm{a}}.\frac{\partial v}{\partial R} \tag{8}$$

$$\gamma_{xz} = \frac{1}{\mathrm{t}}.\frac{\partial u}{\partial s} + \frac{1}{\mathrm{a}}.\frac{\partial w}{\partial R} \tag{9}$$

$$\gamma_{yz} = \frac{1}{\mathrm{t}}.\frac{\partial v}{\partial s} + \frac{1}{\mathrm{a}\beta}.\frac{\partial w}{\partial Q} \tag{10}$$

Where:

$$x = aR \tag{11}$$

$$y = bQ \tag{12}$$

3.3. Constitutive Relations

According to Hooke's law, the 3-D constitutive relation was obtained and result is separated into two equations, one for the normal stress- normal strains relation:

$$\begin{bmatrix}\sigma_x\\ \sigma_y\\ \sigma_z\end{bmatrix} = \frac{\mathrm{E}}{(1+\mu)(1-2\mu)}\begin{bmatrix}(1-\mu) & \mu & \mu\\ \mu & (1-\mu) & \mu\\ \mu & \mu & (1-\mu)\end{bmatrix}\begin{bmatrix}\varepsilon_x\\ \varepsilon_y\\ \varepsilon_z\end{bmatrix} \tag{13}$$

And the other is the for shear stress- shear strains relation:

$$\begin{bmatrix}\tau_{xz}\\ \tau_{yz}\\ \tau_{xy}\end{bmatrix} = \frac{\mathrm{E}}{2(1+\mu)}\begin{bmatrix}\gamma_{xz}\\ \gamma_{yz}\\ \gamma_{xy}\end{bmatrix} \tag{14}$$

The three normal stress components were obtained by substituting Equations 4 to 7 into Equation 13 and

simplifying the outcome as:

$$\sigma_x = \frac{\mathrm{E}}{(1+\mu)(1-2\mu)}\left[(1-\mu)\,\frac{\mathrm{ts}}{\mathrm{a}}.\frac{\partial\theta_{sx}}{\partial R} + \mu\frac{\mathrm{ts}}{\mathrm{a}\beta}.\frac{\partial\theta_{sy}}{\partial Q} + \mu\frac{1}{\mathrm{t}}.\frac{\partial \mathrm{w}}{\partial \mathrm{S}}\right] \quad (15)$$

$$\sigma_y = \frac{\mathrm{E}}{(1+\mu)(1-2\mu)}\left[\mu\mathrm{ts}.\frac{\partial\theta_{sx}}{a\partial R} + \frac{(1-\mu)\mathrm{ts}}{a\beta}.\frac{\partial\,\theta_{sy}}{\partial Q} + \frac{\mu}{t}.\frac{\partial w}{\partial S}\right] \quad (16)$$

$$\sigma_z = \frac{\mathrm{E}}{(1+\mu)(1-2\mu)}\left[\mu\mathrm{ts}.\frac{\partial\theta_{sx}}{a\partial R} + \frac{\mu\mathrm{ts}}{a\beta}.\frac{\partial\,\theta_{sy}}{\partial Q} + \frac{(1-\mu)}{t}.\frac{\partial w}{\partial S}\right] \quad (17)$$

The shear three stress components were obtained by substituting Equations 8 to 10 into Equation 14 and simplifying the outcome as:

$$\tau_{xy} = \frac{E(1-2\mu)}{(1+\mu)(1-2\mu)}.\left[\frac{\mathrm{ts}}{2a\beta}\frac{\partial\theta_{sx}}{\partial Q} + \frac{\mathrm{ts}\partial\,\theta_{sy}}{2a\partial R}\right] \quad (18)$$

$$\tau_{xz} = \frac{(1-2\mu)E}{(1+\mu)(1-2\mu)}.\left[\frac{\theta_{sx}}{2} + \frac{1}{2a}\frac{\partial w}{\partial R}\right] \quad (19)$$

$$\tau_{yz} = \frac{(1-2\mu)E}{(1+\mu)(1-2\mu)}.\left[\frac{\theta_{sy}}{2} + \frac{1}{2a\beta}\frac{\partial w}{\partial Q}\right] \quad (20)$$

3.4. Strain Energy

Strain energy is defined as the average of the product of stress and strain indefinitely summed up within the spatial domain of the body. This mathematically expressed as:

$$U = \frac{abt}{2}\int_0^1\int_0^1\int_{-0.5}^{0.5}\left(\sigma_x\varepsilon_x + \sigma_y\varepsilon_y + \sigma_z\varepsilon_z + \tau_{xy}\gamma_{xy} + \tau_{xz}\gamma_{xz} + \tau_{yz}\gamma_{yz}\right)dR\;dQ\;dS \quad (21)$$

Substituting the values of stresses and strains into Equation 21, and integrate its dot product with respect to dS gives:

$$\begin{aligned}\mathrm{U} = \frac{\mathrm{Et}^3 ab}{24(1+\mu)(1-2\mu)\mathrm{a}^2}\int_0^1\int_0^1\Bigg[&(1-\mu)\left(\frac{\partial\theta_{sx}}{\partial R}\right)^2 + \frac{1}{\beta}\frac{\partial\theta_{sx}}{\partial R}.\frac{\partial\theta_{sy}}{\partial Q} + \frac{(1-\mu)}{\beta^2}\left(\frac{\partial\theta_{sy}}{\partial Q}\right)^2 + \frac{(1-2\mu)}{2\beta^2}\left(\frac{\partial\theta_{sx}}{\partial Q}\right)^2\\ &+\frac{(1-2\mu)}{2}\left(\frac{\partial\theta_{sy}}{\partial R}\right)^2\\ &+\frac{12.(1-2\mu)}{2\mathrm{t}^2}\left(\mathrm{a}^2{\theta_{sx}}^2 + \mathrm{a}^2{\theta_{sy}}^2 + \left(\frac{\partial \mathrm{w}}{\partial R}\right)^2 + \frac{1}{\beta^2}\left(\frac{\partial \mathrm{w}}{\partial Q}\right)^2 + 2\mathrm{a}.\theta_{sx}\frac{\partial \mathrm{w}}{\partial R} + \frac{2\mathrm{a}.\theta_{sy}}{\beta}\frac{\partial \mathrm{w}}{\partial Q}\right) + 0\\ &*2\frac{\mu\mathrm{a}}{\mathrm{t}^2}.\left(\frac{\partial\theta_{sx}}{\partial R}.\frac{\partial \mathrm{w}}{\partial S} + \frac{1}{\beta}.\frac{\partial\theta_{sy}}{\partial Q}.\frac{\partial \mathrm{w}}{\partial S}\right) + \frac{(1-\mu)\mathrm{a}^2}{t^4}\left(\frac{\partial \mathrm{w}}{\partial S}\right)^2\Bigg]\mathrm{dR}\;\mathrm{dQ}\end{aligned} \quad (22)$$

Where:

$$D^* = \frac{Et^3}{12(1+\mu)(1-2\mu)} \quad (23)$$

3.5. Energy Equation Formulation

Total Energy Expression be the algebraic summation of strain energy (U) and external work (V). That is:

$$\prod = \mathrm{U} - \mathrm{V} \quad (24)$$

$$V = abqA_1\int_0^1\int_0^1 h\,dR\;dQ \quad (25)$$

Substituting Equations 22 and 25 into Equation 24 gives:

$$\Pi = \frac{D^* ab}{2a^2}\int_0^1\int_0^1\left[(1-\mu)\left(\frac{\partial\theta_{sx}}{\partial R}\right)^2 + \frac{1}{\beta}\frac{\partial\theta_{sx}}{\partial R}.\frac{\partial\theta_{sy}}{\partial Q} + \frac{(1-\mu)}{\beta^2}\left(\frac{\partial\theta_{sy}}{\partial Q}\right)^2 + \frac{(1-2\mu)}{2\beta^2}\left(\frac{\partial\theta_{sx}}{\partial Q}\right)^2 + \frac{(1-2\mu)}{2}\left(\frac{\partial\theta_{sy}}{\partial R}\right)^2 + \frac{6(1-2\mu)}{t^2}\left(a^2{\theta_{sx}}^2 + a^2{\theta_{sy}}^2 + \left(\frac{\partial w}{\partial R}\right)^2 + \frac{1}{\beta^2}\left(\frac{\partial w}{\partial Q}\right)^2 + 2a.\theta_{sx}\frac{\partial w}{\partial R} + \frac{2a.\theta_{sy}}{\beta}\frac{\partial w}{\partial Q}\right) + \frac{(1-\mu)a^2}{t^4}\left(\frac{\partial w}{\partial S}\right)^2\right]dR\,dQ - \int_0^1\int_0^1 abqhA_1\partial R\partial Q \quad (26)$$

3.6. Governing Equation

The solution of the governing equation in trigonometric form is obtained in line with the work of Onyeka, *et al.* [34] by minimizing the total potential energy functional with respect to deflection to give the exact deflection equation, shear deformation rotation in x-axis and shear deformation rotation in y-axis as presented in Equation 27, 28 and 29 respectively:

$$h = [1 \quad R \quad Cos\,(c_1R) \quad Sin\,(c_1R)]\begin{bmatrix}a_0\\a_1\\a_2\\a_3\end{bmatrix}.[1 \quad Q \quad Cos\,(c_1Q) \quad Sin\,(c_1Q)]\begin{bmatrix}b_0\\b_1\\b_2\\b_3\end{bmatrix}/A_1 \quad (27)$$

$$\theta_{sx} = \frac{c}{a}.\Delta_0.[1 \quad c_1Sin\,(c_1R) \quad c_1Cos\,(c_1R)]\begin{bmatrix}a_1\\a_2\\a_3\end{bmatrix}.[1 \quad Q \quad Cos\,(c_1Q) \quad Sin\,(c_1Q)]\begin{bmatrix}b_0\\b_1\\b_2\\b_3\end{bmatrix} \quad (28)$$

$$\theta_{sy} = \frac{c}{a\beta}.\Delta_0.[1 \quad R \quad Cos\,(c_1R) \quad Sin\,(c_1R)]\begin{bmatrix}a_0\\a_1\\a_2\\a_3\end{bmatrix}.[1 \quad c_1Sin\,(c_1Q) \quad c_1Cos\,(c_1Q)]\begin{bmatrix}b_1\\b_2\\b_3\end{bmatrix} \quad (29)$$

Let:

$$w = A_1.h \quad (30)$$

$$\theta_{sx} = \frac{A_2}{a}.\frac{\partial h}{\partial R} \quad (31)$$

$$\theta_{sy} = \frac{A_3}{a\beta}.\frac{\partial h}{\partial Q} \quad (32)$$

Substituting Equation 30, 31 and 32 into 26, gives:

$$\Pi = \frac{D^* ab}{2a^4}\left[(1-\mu){A_2}^2k_x + \frac{1}{\beta^2}\left[A_2.A_3 + \frac{(1-2\mu){A_2}^2}{2} + \frac{(1-2\mu){A_3}^2}{2}\right]k_{xy} + \frac{(1-\mu){A_3}^2}{\beta^4}k_y + 6(1-2\mu)\left(\frac{a}{t}\right)^2\left(\left[{A_2}^2 + {A_1}^2 + 2A_1A_2\right].k_z + \frac{1}{\beta^2}.\left[{A_3}^2 + {A_1}^2 + 2A_1A_3\right].k_{2z}\right) - \frac{2qa^4k_hA_1}{D^*}\right] \quad (33)$$

Minimizing Equation 33 with respect to A_2 gives:

$$\frac{\partial\Pi}{\partial A_2} = (1-\mu)A_2k_x + \frac{1}{2\beta^2}[A_3 + A_2(1-2\mu)]k_{xy} + 6(1-2\mu)\left(\frac{a}{t}\right)^2[A_2 + A_1].k_z = 0 \quad (34)$$

Minimizing Equation 33 with respect to A_3 gives:

$$\frac{\partial\Pi}{\partial A_2} = \frac{(1-\mu)A_3}{\beta^4}k_y + \frac{1}{2\beta^2}[A_2 + A_3(1-2\mu)]k_{xy} + \frac{6}{\beta^2}(1-2\mu)\left(\frac{a}{t}\right)^2([A_3 + A_1].k_{2z}) = 0 \quad (35)$$

Rewriting Equations 34 and 35 gives:

$$\left[(1-\mu)k_x + \frac{1}{2\beta^2}(1-2\mu)k_{xy} + 6(1-2\mu)\left(\frac{a}{t}\right)^2k_z\right]A_2 + \left[\frac{1}{2\beta^2}k_{xy}\right]A_3 = \left[-6(1-2\mu)\left(\frac{a}{t}\right)^2k_z\right]A_1 \quad (36)$$

$$\left[\frac{1}{2\beta^2}k_{xy}\right]A_2+\left[\frac{(1-\mu)}{\beta^4}k_y+\frac{1}{2\beta^2}(1-2\mu)k_{xy}+\frac{6}{\beta^2}(1-2\mu)\left(\frac{a}{t}\right)^2k_{2z}\right]A_3$$
$$=\left[-\frac{6}{\beta^2}(1-2\mu)\left(\frac{a}{t}\right)^2k_Q\right]A_1 \quad (37)$$

Solving Equations 36 and 37 simultaneously gives:

$$A_2=MA_1 \quad (38)$$
$$A_3=NA_1 \quad (39)$$

Let:

$$M=\frac{(r_{12}r_{23}-r_{13}r_{22})}{(r_{12}r_{12}-r_{11}r_{22})} \quad (40)$$
$$N=\frac{(r_{12}r_{13}-r_{11}r_{23})}{(r_{12}r_{12}-r_{11}r_{22})} \quad (41)$$

Where:

$$r_{11}=(1-\mu)k_x+\frac{1}{2\beta^2}(1-2\mu)k_{xy}+6(1-2\mu)\left(\frac{a}{t}\right)^2k_z \quad (42)$$
$$r_{22}=\frac{(1-\mu)}{\beta^4}k_y+\frac{1}{2\beta^2}(1-2\mu)k_{xy}+\frac{6}{\beta^2}(1-2\mu)\left(\frac{a}{t}\right)^2k_{2z} \quad (43)$$
$$r_{12}=r_{21}=\frac{1}{2\beta^2}k_{xy};\ r_{13}=-6(1-2\mu)\left(\frac{a}{t}\right)^2k_z;\ r_{23}=r_{32}=-\frac{6}{\beta^2}(1-2\mu)\left(\frac{a}{t}\right)^2k_{2z} \quad (44)$$

Minimizing Equation 33 with respect to A_1 gives:

$$\frac{\partial\Pi}{\partial A_1}=\frac{D^*ab}{2a^4}\left[6(1-2\mu)\left(\frac{a}{t}\right)^2\left([2A_1+2A_2].k_z+\frac{1}{\beta^2}.[2A_1+2A_3].k_{2z}\right)-\frac{2qa^4k_h}{D^*}\right]=0 \quad (45)$$

That is:

$$6(1-2\mu)\left(\frac{a}{t}\right)^2\left([A_1+UA_1].k_z+\frac{1}{\beta^2}.[A_1+VA_1].k_{2z}\right)-\frac{qa^4k_h}{D^*}=0 \quad (46)$$

Factorizing Equations (46) and simplifying gives:

$$6(1-2\mu)\left(\frac{a}{t}\right)^2A_1\left([1+U].k_z+\frac{1}{\beta^2}.[1+V].k_{2z}\right)=\frac{qa^4k_h}{D^*} \quad (47)$$
$$TA_1=\frac{qa^4k_h}{D^*} \quad (48)$$
$$A_1=\frac{qa^4}{D^*}\left(\frac{k_h}{T}\right) \quad (49)$$

Where:

$$T=6(1-2\mu)\left(\frac{a}{t}\right)^2*\left([1+U].k_z+\frac{1}{\beta^2}.[1+V].k_{2z}\right) \quad (50)$$

3.7. Numerical Analysis

The numerical analysis of a rectangular thick plate whose Poisson's ratio is 0.3 under CSCS boundary conditions as shown in the Figure 4 and carrying uniformly distributed load (including self-weight) is presented. An exact trigonometric function as was obtained in the Equation 27 and applied here to get the actual values of the shape functions, coefficients of deflection and shear deformation rotations at x and y axis of the plate.

The boundary conditions of the plate in Figure 3 are as follows:

R- Direction

(a) When R = 0, deflection (w) = 0. (51)

(b) When R = 0, bending moment (w'') = 0, $\left(ie.\frac{d^2w}{dR^2}=0\right)$ (52)

(c) When R = 1, deflection (w) = 0. (53)

d) When R = 1, bending moment = 0, $\left(ie.\frac{d^2w}{dR^2}=0\right)$ (54)

Q - Direction

(e) When Q = 0, deflection (w) = 0. (55)

(f) When Q = 0, slope (w') = 0, $\left(ie.\frac{dw}{dQ}=0\right)$ (56)

(g) When Q = 1, deflection (w) = 0. (57)

(h) When Q = 1, slope (w') = 0, $\left(ie.\frac{dw}{dQ}=0\right)$ (58)

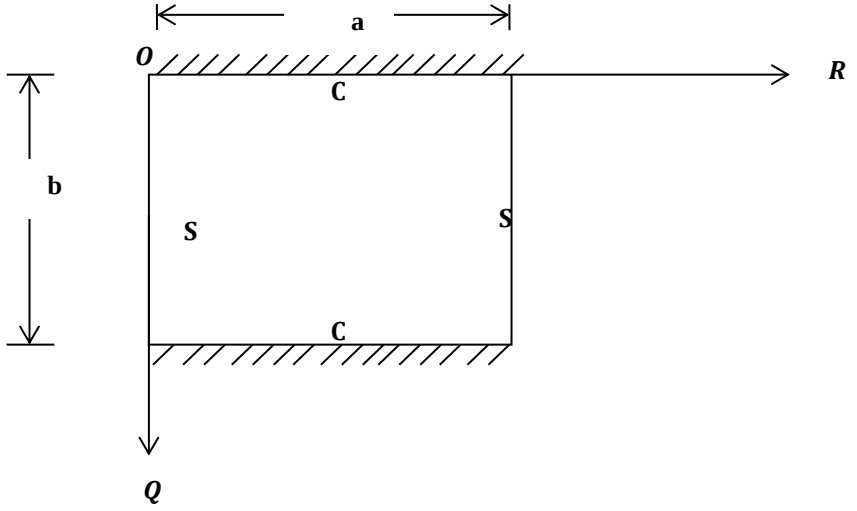

Fig 3: CSCS rectangular plate

The derived trigonometric deflection $w\ (x,y)$ functions is subjected to a CSCS boundary condition to get the particular solution of the deflection. This can be achieved by substituting the following boundary conditions into Equations (51) to (58) and solving for the equation gave non-trivial solution as:

$sing_1 = 0;\ 2Cos\ g_1 + g_1\ Sin\ g_1 - 2 = 0$ (59)

The value of g_1 that satisfies Equation (59) is:

$g_1 = m\pi\ ; g_1 = 2m\pi\ [where\ m = n = 1, 2, 3\ ...]$ (60)

Substituting Equation (60) into derivatives of Equation (27) and satisfying the boundary conditions of Equations (51) to (58) gave;

$a_0 = a_1 = a_2;\ \ b_1 = b_3 = 0;\ b_0 = -b_2 = 0$ (61)

Substituting the constants of Equation (60) and (61) into Equation (27) gave;

$w = a_3 Sin(m\ \pi R.).b_2(Cos2n\pi Q - 1)$ (62)

Recall;

$w = h.A_1$

Let $m = n = 1$

Therefore:

$w\ = a_3.b_2(Sin\ \pi R).(Cos\ 2\pi Q - 1)$ (63)

Let the amplitude,

$A_1 = a_3.b_2$ (64)

And the shape function of the plate be:

$h = Sin\ \pi R.(Cos\ 2\pi Q - 1)$ (65)

Thus, the exact trigonometric deflection $w\ (x,y)$ functions under CSCS boundary condition becomes:

$w = (Sin\ \pi R).(Cos2\pi Q - 1)A_1$ (66)

Table 1: Trigonometric form of stiffness coefficients of CCCC rectangular plate

Deflection form	k_x	k_{xy}	k_y	k_z	k_{2z}	k_h
Trigonometry	$\frac{3\pi^4}{4}$	π^4	$4\pi^4$	$\frac{3\pi^2}{4}$	$\frac{\pi^2}{4}$	$\frac{2}{\pi}$

3.8. Exact Displacement and Stress Expression

The value of A_1 A_2, A_3 in Equation (30) or (49), (31) or (38) and (32) or (39) is substituted into Equation 1 and 2 where appropriate to get the in-plane displacement along x-axis becomes:

$$u = ts.\frac{M}{a}.\frac{qa^4}{D^*}\left(\frac{k_h}{T}\right)\frac{\partial h}{\partial R} \tag{67}$$

And the in-plane displacement along y-axis becomes

$$v = ts.\frac{N}{a\beta}.\frac{qa^4}{D^*}\left(\frac{k_h}{T}\right)\frac{\partial h}{\partial Q} \tag{68}$$

Substitute Equation 49 into Equation 66, the deflection equation of the plate becomes:

$$w = (\,Cos2\pi R - 1).(Cos2\pi Q - 1).\frac{qa^4}{D^*}\left(\frac{k_h}{T}\right) \tag{69}$$

The value of A_1, A_2 and A_3 Equation (30) or (49), (31) and (32) is substituted into Equation 15 -17 where appropriate to get the three normal stress elements as:

$$\sigma_x = \frac{\mathrm{E}}{(1+\mu)(1-2\mu)}\left[(1-\mu)\,\frac{\mathrm{ts}}{\mathrm{a}}.\frac{\partial^2 h}{\partial R^2}A_2 + \mu\frac{\mathrm{ts}}{\mathrm{a}\beta}.\frac{\partial^2 h}{\partial Q^2}A_3 + \mu\frac{1}{\mathrm{t}}.\frac{qa^4}{D^*}\left(\frac{k_h}{T}\right)\frac{\partial \mathrm{h}}{\partial \mathrm{S}}A_1\right] \tag{70}$$

$$\sigma_y = \frac{\mathrm{E}}{(1+\mu)(1-2\mu)}\left[\frac{\mu\mathrm{ts}}{a}.\frac{\partial^2 h}{\partial R^2}A_2 + \frac{(1-\mu)\mathrm{ts}}{a\beta}.\frac{\partial^2 h}{\partial Q^2}A_2 + \frac{\mu}{t}.\frac{qa^4}{D^*}\left(\frac{k_h}{T}\right)\frac{\partial \mathrm{h}}{\partial \mathrm{S}}A_1\right] \tag{71}$$

$$\sigma_z = \frac{\mathrm{E}}{(1+\mu)(1-2\mu)}\left[\frac{\mu\mathrm{ts}}{a}.\frac{\partial^2 h}{\partial R^2}A_2 + \frac{\mu\mathrm{ts}}{a\beta}.\frac{\partial^2 h}{\partial Q^2}A_3 + \frac{(1-\mu)}{t}.\frac{qa^4}{D^*}\left(\frac{k_h}{T}\right)\frac{\partial \mathrm{h}}{\partial \mathrm{S}}A_4\right] \tag{72}$$

The value of A_1, A_2 and A_3 in Equation (30) or (49), (31) and (32) is substituted into Equation 18 -20 where appropriate to get the three shear stress elements as:

$$\tau_{xy} = \frac{E(1-2\mu)}{(1+\mu)(1-2\mu)}.\left[\frac{\mathrm{ts}}{2a\beta}.\frac{\partial^2}{\partial R\,\partial Q}A_2 + \frac{\mathrm{ts}}{2a}.\frac{\partial^2}{\partial R\,\partial Q}A_3\right] \tag{73}$$

$$\tau_{xz} = \frac{(1-2\mu)E}{(1+\mu)(1-2\mu)}.\left[\frac{A_2}{2a}\frac{\partial \mathrm{h}}{\partial R} + \frac{1}{2a}.\frac{qa^4}{D^*}\left(\frac{k_h}{T}\right)\frac{\partial h}{\partial R}\right] \tag{74}$$

$$\tau_{yz} = \frac{(1-2\mu)E}{(1+\mu)(1-2\mu)}.\left[\frac{A_2}{2a}\frac{\partial \mathrm{h}}{\partial Q} + \frac{1}{2a\beta}.\frac{qa^4}{D^*}\left(\frac{k_h}{T}\right)\frac{\partial h}{\partial Q}\right] \tag{75}$$

3.8. Exact Bending Moment Expression of the Plate

The bending moment in the direction of the main reinforcement of the plate is established by determining the relationship between the established deflection and moment using the Hooke's law principle by considering shear deformation effect as:

$$M_x = D^*\left[\left(\frac{\partial^2 w}{\partial x^2} + \mu\frac{\partial^2 w}{\partial y^2}\right) + \left(\frac{\partial \theta_{Sx}}{\partial x} + \mu\frac{\partial \theta_{Sy}}{\partial y}\right)\right] \tag{76}$$

Thus:

$$M_x = \frac{Et^3}{12(1+\mu)(1-2\mu)}\left[\frac{A_1}{a^2}\left(\frac{\partial^2 h}{\partial R^2} + \frac{\mu}{\beta^2}\frac{\partial^2 h}{\partial Q^2}\right) + \left(\frac{A_2}{a}\frac{\partial h}{\partial R} + \mu\frac{A_3}{a\beta}\frac{\partial h}{\partial Q}\right)\right] \tag{77}$$

Similarly:

$$M_y = D^*\left[\left(\frac{\partial^2 w}{\partial y^2} + \mu\frac{\partial^2 w}{\partial x^2}\right) + \left(\frac{\partial \theta_{Sy}}{\partial y} + \mu\frac{\partial \theta_{Sx}}{\partial x}\right)\right] \tag{78}$$

Thus:

$$M_y = \frac{Et^3}{12(1+\mu)(1-2\mu)}\left[\frac{A_1}{a^2}\left(\frac{\partial^2 h}{\beta^2\partial Q^2} + \mu\frac{\partial^2 h}{\partial R^2}\right) + \left(\frac{A_3}{a\beta}\frac{\partial h}{\partial Q} + \mu\frac{A_2}{a}\frac{\partial h}{\partial R}\right)\right] \tag{79}$$

4. Results and Discussions

A parametric data for the trigonometric stiffness coefficient, k_x, k_{xy}, k_y, k_z, k_{2z} and k_q for CSCS shape functions is presented in Table 1. The Equation for different coefficient can be found in the nomenclature section and a graph representing its numerical values can be found in the Figure 4. This stiffness coefficients were used to obtain the value of the shape functions, coefficient of deflection and rotation of the plate material when subjected to a

uniformly distributed transverse load under the same boundary conditions. The theoretical interpretation of the plate as regards to its performance and boundary condition showed that it is a rectangular plate which is clamped and simply supported at the two opposite edges (CSCS). This depicts that the plate was clamped at the first edge towards right, simply supported at the third edges while the second and fourth edges of the plate were simply supported. The physical description of the plate's model showed that, the two clamped edges are supported by a column and continuous over the span of the plate while the remaining two edges are supported by a beam and situated adjacent towards the other clamped supported edge. This makes the study very significant because such boundary condition exist depending on the type of beam/column support in the plate structure. So, whenever a case of such support exists in the structure, analysing the plate as if is any other boundary e.g. CCCC, will not account for all the forces (stresses) acting on it. This is because, forces are generated due to the applied load on the structure thereby will introduce significant errors in the analysis and not predict an accurate or reliable result for the design if they are not considered. Thus, for a safe structural design of plate (slab) in a building or any type of structure with CSCS boundary conditions (BCs), plate analysis with CSCS BCs like this is required.

The present work obtained non-dimensional result of displacement, moment and the stresses of the plate by expressing the deflection and rotation functions of the plate in the form of trigonometry to analyse the effect of aspect ratio of the bending characteristics of the plate. The graph in Figure 5 showed that k_y and k_{xy} are having the highest coefficient followed by k_x while $k_{2z,}$ k_z and k_q contains the lowest amount of stiffness coefficient. The numerical results of the non-dimensional displacements (u, v & w) and the stresses characteristics of a 3-D clamped rectangular plate which was subjected to uniform distributed load was obtained using the established exact trigonometric displacement function.

Fig 4: Stiffness coefficient for the CSCS plate boundary condition

A graphic representation of results of the non-dimensional value of bending moment coefficient of a square thick rectangular plate while Table 2 and 3 contains the displacements, normal stresses and shear stresses of the plate at different span-thickness aspect ratio. Hence, for the purpose of result discussion, only the square is considered for the numeric values of bending moment of this study while the stress and displace analysis is presented in the aspect ratio of 1 and 1.5 respectively.

The numerical comparative analysis was presented to show the disparities between the present study and the literature under review to show the effect of aspect ratio on the 3-D bending, deformation and stress analysis of rectangular plate at varying aspect ratio. The span-thickness ratio considered is ranged between 4, 5, 10, 15, 20, 50, 100 and CPT, which is obviously seen to span from the thick plate, moderately thick plate and thin plate [34]. Table 4 showed the results of the numerical analysis performed for the span-thickness ratio of 4, 5 and 10 while Table 5 showed the results of the numerical analysis performed for the aspect ratio of 5 and 10 respectively.

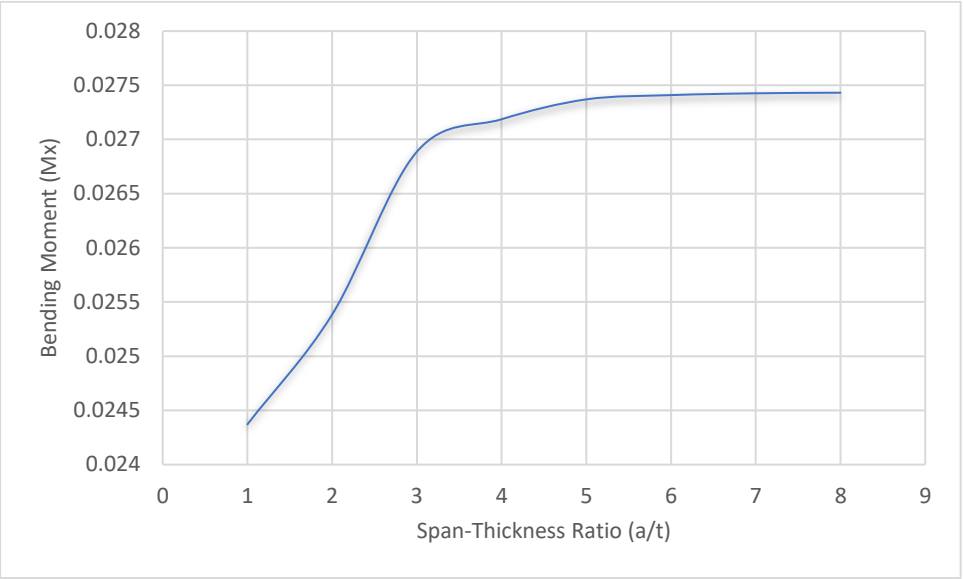

Fig. 5: Graph of Bending Moment versus Span-thickness ratio of the plate

The graph in the Figure 5 showed that as the aspect ratio of the plate increase, the bending moment along x and y coordinates (M_x and M_y) decrease. This is quite expected because the relationship between the bending moment and the deflection in the plate section. Thus, the deflection (w) which occurs at the plate due to the applied load increase with increases in the value of the span-thickness ratio of the plate. This implies that, the span-bending curvature increase causes deflection in the mid-plane of the plate.

Table 2: The result of displacements and stresses of a CSCS aspect ratio of 1.0

$\beta = \frac{a}{t}$	w	u	v	σ_x	σ_y	σ_z	τ_{xy}	τ_{xz}	τ_{yz}
4	0.00220	-0.00255	-0.00351	0.17302	0.24402	0.17062	-0.0864	0.00622	0.00198
5	0.00208	-0.00258	-0.0034	0.17193	0.23703	0.16953	-0.0853	0.00405	0.00120
10	0.00192	-0.00262	-0.00323	0.17084	0.22736	0.16844	-0.0838	0.00097	0.00020
15	0.00189	-0.00263	-0.00320	0.17070	0.22552	0.16830	-0.0835	0.00037	0.00023
30	0.00187	-0.00264	-0.00318	0.17060	0.22441	0.16820	-0.0833	0.00002	-0.0001
50	0.00187	-0.00264	-0.00318	0.17060	0.22417	0.16820	-0.0833	-0.0001	-0.0001
100	0.00187	-0.00264	-0.00318	0.17059	0.22407	0.16819	-0.0833	-0.0001	-0.0001
CPT	0.00187	-0.00264	-0.00317	0.17059	0.22403	0.16819	-0.0833	-0.0001	-0.0001

The non-dimensional result in the Tables 2 shows that as the span-thickness ratio of the plate increase, the in-plane displacement along x and y axis (u and v) increases too, whereas, the deflection (w) which occurs at the plate due to the applied load decrease with increases in the value of the span-thickness ratio of the plate. On the other hand, the stress perpendicular to the x, y and z axis (σ_x, σ_y & σ_z) decreases as the span-depth ratio of the plate increases. Meanwhile, the increase at the span-thickness ratio of the plate increases the value shear stress along the x-y (τ_{xy}) while the span - depth ratio causes a decrease in the value shear stress along the x-z and y-z plane (τ_{xz} & τ_{yz}). These decreases continue until the plate structure deflects beyond the elastic yield stress, hence, failure occurs.

Table 2 shows that, at a span - depth ratio between 4 and 30, the value of deflection varies between 0.00208 and 0.00187. At the span - depth ratio 30 and above, a constant value of 0.00187 is noticed, this value is equal to the value of the CPT. This is quite expected since we assumed in CPT analyses that at span-thickness ratios of 100 and above, a plate can be taken as being thin. Similarly, it can be seen that, at a span - depth ratio between 4 and 30, the non-dimensional value of transverse shear stress along y-z coordinates varies between 0.00198 and -0.0001. The value of transverse shear stress along y-z coordinates being less than or equal the value showed that this value is the same as that of CPT. This constant value of -0.0001 from 30 and above confirmed the finding in the value of deflection obtained. It can be deduced that the value of deflection and shear stress varies more as the plate is thicker and vary

less as the span - depth increase (thinner plate) under the same loading capacity/condition. It can be said that at a span - depth ratio between 4 and 30 the plate is regarded as thick. The span - thickness ratio of 30 and beyond, the plate is regarded as thin or moderately thick because its value at this point coincides with the value of the CPT.

Table 3: Displacement and stresses of a CSCS plate aspect ratio of 1.5

$\beta = \frac{a}{t}$	w	u	v	σ_x	σ_y	σ_z	τ_{xy}	τ_{xz}	τ_{yz}
4	0.00626	-0.00716	-0.00648	0.39975	0.36024	0.35784	0.01263	0.01263	0.00205
5	0.00595	-0.00712	-0.00623	0.39505	0.34934	0.34694	0.00816	0.00816	0.00124
10	0.00553	-0.00711	-0.00588	0.38892	0.33438	0.33198	0.00199	0.00199	0.00021
15	0.00546	-0.00711	-0.00582	0.3878	0.33156	0.32916	0.00082	0.00082	0.00026
30	0.00541	-0.00711	-0.00578	0.38714	0.32985	0.32745	-0.1521	0.00012	-0.0001
50	0.00540	-0.00711	-0.00577	0.38699	0.32949	0.32709	-0.1519	-0.0000	-0.0001
100	0.00539	-0.00711	-0.00577	0.38693	0.32934	0.32694	-0.1519	-0.0000	-0.0001
CPT	0.00539	-0.00716	-0.00577	0.38691	0.32928	0.32688	-0.1519	-0.0000	-0.0001

The non-dimensional result in the Tables 3 shows that as the span-thickness ratio of the plate increase, the in-plane displacement along x and y axis (u and v) increases too, whereas, the deflection (w) which occurs at the plate due to the applied load decrease with increases in the value of the span-thickness ratio of the plate. On the other hand, the stress perpendicular to the x, y and z axis (σ_x, σ_y & σ_z) decreases as the span-depth ratio of the plate increases. Meanwhile, the increase at the span-thickness ratio of the plate increases the value shear stress along the x-y plane (τ_{xy}) while the span - depth ratio causes a decrease in the value shear stress along the x-z and y-z plane (τ_{xz} & τ_{yz}). These decrease continue until the plate structure deflects beyond the elastic yield stress, hence, failure occurs.

Table 3 shows that, at a span - depth ratio between 4 and 30, the value of deflection varies between 0.0063 and 0.0054. At the span - depth ratio 30 and above, a constant value of 0.0054 is noticed, this value is equal to the value of the CPT. This is quite expected since we assumed in CPT analyses that at span-thickness ratios of 100 and above, a plate can be taken as being thin. Similarly, it can be seen that, at a span - depth ratio between 4 and 30, the non-dimensional value of transverse shear stress along y-z coordinates varies between 0.00198 and -0.001. The value of transverse shear stress along y-z coordinates being less than or equal the value showed that this value is the same as that of CPT. This constant value of -0.0001 from 30 and above confirmed the finding in the value of deflection obtained. It can be deduced that the value of deflection and shear stress varies more as the plate is thicker and vary less as the span - depth increase (thinner plate) under the same loading capacity/condition. It can be said that at a span - depth ratio between 4 and 30 the plate is regarded as thick. The span - thickness ratio of 30 and beyond, the plate is regarded as thin or moderately thick because its value at this point coincides with the value of the CPT.

Study in the Table 2 and 3 shows that as the aspect ratio of the plate increase, the in-plane displacement along x and y axis (u and v) decrease whereas, the deflection (w) which occurs in the plate due to the applied load increase with increases in the value of the span-thickness ratio of the plate. On the other hand, the stress perpendicular to the x, y and z axis increases as the span-depth ratio of the plate increases. This implies that, as the length of the plate material increases, more stresses are induced in the plate which consequently leads to the failure of the plate material if the plate material are stretched beyond the elastic limit. This means that the failure in a plate structure is bound to occur as the more stresses are induced within the plate element which affects the performance in terms of the serviceability of the plate. Thus, caution must be taken when selecting the depth and other dimensions along the x and y co-ordinate of the plate to ensure accuracy of the analysis and safety in the construction.

Table 4: Comparative deflection analysis for square plate at varying span-thickness ratio (β = a/t) between present study and past studies

$\beta = \frac{a}{t}$	Present Study	Onyeka *et al.* [35]	Wang *et al.* [90]	Reddy [91]
4	0.00626	-0.00716	-0.00648	0.39975
5	0.00595	-0.00712	-0.00623	0.39505
10	0.00553	-0.00711	-0.00588	0.38892

In summary, there are three categories of rectangular plates. The plates whose deflection and vertical shear stress do not vary much with CPT is categorized as thin plate. Hence, the plate whose deflection and transverse shear stress varies very much from zero is categorized as thick plates. Thus, the span-thickness ratio for these categories of

rectangular plates are: Thick plate is categorized as the plate with the span to thickness ratio: $a/t \leq 30$ while the thin or the moderately thick plate is categorized as the plate with the span to thickness ratio: $a/t \geq 30$. Meanwhile, the present theory stress prediction shows that the result of the displacement and stress of thin and moderately thick plate using the 3-D theory is the same for the bending analysis of rectangular plate under the CSCS boundary condition.

Table 5: Non-dimensional values bending moment for CSCS square plate from different scholars [35, 44, 41 and 43]

$\beta = \frac{a}{t}$	Point (a/x, b/y)	Present Study	Onyeka *et al.* [35]	Xiao *et al.* [44]	Kant & Hinton [41]	Lee *et al.* [43]
5	(0.5,0.5)	0.0275	0.0281	0.0299	0.0292	0.0292
10	(0.5,0.5)	0.0274	0.0266	0.0255	0.0258	0.0258

The result of comparative analysis performed in the Table 4 and 5 showed the disparity between different theories used in the plate analysis especially as it concerns thick plate. This theory includes the analytical and numerical process of RPT using different approaches. A percentage difference evaluation was adopted as presented in Table 6 to compare and show the validity of the derived relationships in the deflection analysis. The result of percentage difference evaluation in Table 6 showed that the plate with the largest thickness (a/t of 4) gives a percentage difference of 0.551% between the present study and the work of Onyeka *et al.* [34]. There is no deflection result available in the literature for the work of Reddy [9], therefore the percentage difference evaluation with the present study could not be determined. On the other hand, the result percentage difference analysis between the present study and the work of Onyeka *et al.* [34], Wang *et al.* [90] and Reddy [9] at span-depth ratio of 5 is 5.140%, 26.532% and 37.456% respectively. More, so, the plate at 10 span-depth ratio gives a percentage difference of 5.731%, 2.367% and 6.212% of the work [34], Reddy [9], when compared with the present study.

Table 5 showed that, the percentage difference between the present study and Reddy [9] in deflection analysis, decreases as the plate is getting thinner while the percentage difference between the present study and Onyeka *et al.* [34], increases as the plate is getting thinner. This shows that the HSDT is best suitable for thick plate ($\frac{a}{t} \geq 30$), unlike the FSDT as it includes shear correction factor which made transverse shear stress variation not uniformly distributed. The calculated average percentage difference between the present study and the work of Onyeka *et al.* [34], Reddy [9] is 5.67%, 14.45% and 21.83%. The small difference the work of Onyeka *et al.* [34]when compare with present exact 3-D theory is quite expected because they used HSDT with a derived deflection function from the elasticity principle which make their solution close-form whereas Reddy [9] used an assumed deflection function which give higher difference when compare with exact 3-D theory of elasticity (Present study). The total average difference between the present study and exact HSDT [34] and FSDT is 5.7% and 18.1%. It can be deduced that the present study using 3-D theory proved the exactness of the theory and derived relationship because of its small difference of 5.7% with the derived RPT, a value which could be negligible in the statically analysis. On the other hand, the difference of 18% which is too high show that the theory used by Reddy [9] over predict the deflection that may occur due to external load on the structure which proved that their theory is in-exact and therefore unreliable for thick plate analysis under such loading and boundary condition.

Table 6: Percentage difference between the present study and work of authors in [34], and [9]

Percentage (%) Difference Evaluation		
$\beta = \frac{a}{t}$	Onyeka *et al.* [34]	Reddy [9]
4	0.551	-
5	5.140	37.456
10	5.731	6.212
Average % Difference	5.67	21.83
Total Ave.% Difference	5.7	18.1
Overall Total Ave.% Difference		11.9

A percentage difference evaluation was adopted as presented in Table 6 to compare and show the validity of the derived relationships in the deflection analysis. The result of percentage difference evaluation in Table 6 showed that the plate with the largest thickness (a/t of 5) gives a percentage difference of 0.551% between the present study and the work of Onyeka *et al.* [35], Xiao *et al.* [92], Kant & Hinton [93] and Lee *et al.* [94] is 2.18%, 8.727%, 6.18 and 6.18%. On the other hand, at the span-depth ratio of 10, the result percentage difference analysis between the present

study and the work of Onyeka *et al.* [35], Xiao *et al.* [92], Kant & Hinton [93] and Lee *et al.* [94] is 2.92%, 6.93%, 5.84%, 5.84% and 6.18% respectively. It is observed that the percentage different between the present study and those of Kant & Hinton [93] and Lee *et al.* [94] are the same that all the span – depth ratio in consideration; this is quite expected as both authors used a numerical method. The average percentage different between the present and both [93, 94] is 6.10.

Table 6 showed that, the percentage difference between the present study and Xiao *et al.* [92], Kant & Hinton [93] and Lee *et al.* [94] in bending moment analysis, decreases as the plate is getting thinner while the percentage difference between the present study and Onyeka *et al.* [35], increases as the plate is getting thinner. This shows that the HSDT with derived deflection function is best suitable for thick plate ($\frac{a}{t} \geq 30$), unlike the HSDT with assumed displacement [92], Numeric Mindlin theory [93] and Levy [94] whose transverse shear stress variation not uniformly distributed.

The calculated average percentage difference between the present study and the work of Onyeka *et al.* [35], Xiao *et al.* [92], Kant & Hinton [93] and Lee *et al.* [94] is 2.55%, 7.83%, 6.01% and 6.01%%. The small difference the work of Onyeka *et al.* [35] when compared with present exact 3-D theory is quite expected because they used HSDT with a derived deflection function from the elasticity principle which make their solution close-form whereas Xiao *et al.* [92], used an HSDT assumed deflection function which give higher difference when compare with the exact 3-D theory of elasticity (Present study).

Table 7: Percentage difference between the present study and work of authors in [35, 92-94]

Percentage (%) Difference Evaluation				
$\beta = \frac{a}{t}$	Onyeka *et al.* [35]	Xiao *et al.* [92]	Kant & Hinton [93]	Lee *et al.* [94]
5	2.182	8.727	6.182	6.182
10	2.920	6.934	5.839	5.839
Average % Difference	2.55	7.83	6.01	6.01
Total Ave.% Difference		5.6		

The total average difference between the present study and exact HSDT [35] and 2-D HSDT with assumed function is 2.55% and 7.83%. This showed that the deflection function when derived from the principle of elasticity give a close-form solution. It can be deduced that the present study using 3-D theory proved the exactness of the theory and derived relationship because of its small difference of 7.83% with the derived RPT, a value which could be negligible in the statically analysis. On the other hand, the difference of 7.83%, which is too high show that the theory used by Xiao *et al.* [92] and Numerical approach [93, 94] over predict the deflection that may occur due to external load on the structure, which proved that their theory is inexact and therefore unreliable for thick plate analysis under such loading and boundary condition.

However, the overall average percentage difference between the present study and those of 2-D HSDT [35, 92] is about 5.19%, the difference being less than or equal than 5% is acceptable in the statically analysis as the same. Meanwhile, the overall average percentage difference between the present study and those of the 2-D numeric analysis [93, 94] is about 6.01%, the difference being more than 5% is not acceptable as it shows a clear difference which means that numerical analysis is an approximate method as they over-predict the moment which causes bending of the plate section. Furthermore, the overall average percentage difference values of moment of the present theory and those of Onyeka *et al.* [35], Xiao *et al.* [92], Kant & Hinton [93] and Lee *et al.* [94] is 5.6%. This showed that at the 94 % confidence level, both theory and methods are the same for a thick plate analysis.

It is worth to note that the 2-D RPT with exact deflection gives a closer result when compared with exact 3-D plate theory than those 2-D RPT with an assumed deflection and other RPT and CPT in the thick plate analysis. Meanwhile, the values predicted by the present theory are in close relationship with previous scholars [35, 92]. The slightly higher average percentage difference of 2.55% showed the coarseness of RPT in the plate analysis because of over-predicting the stresses in the plate. Hence, exact 3-D theory is required to achieve efficiency.

Thus, the present model using the six stress elements to yield the exact solution for the analysis of thick plate that is clamped supported at opposite edges and the other edges simply supported (CSCS). Hence, the result of the present analysis, which contains all the stress element with an exact deflection function ensured that the variation of the stresses through the thickness of the plate which induced stresses can be used in confidence for bending analysis of plate.

4. Conclusion

The 3-D bending and stress analysis of thick rectangular plate using 3-D elasticity theory has been investigated. From the study, the following important points has been drawn:

i. Trigonometric shape function predicts a close-form solution than polynomial displacement function.
ii. The present theory stress prediction shows that the result of the displacement and stress of thin and moderately thick plate using the 3-D theory is the same at span-thickness ratio beyond 50% for the bending analysis of rectangular plate under the CSCS boundary condition.
iii. Plate analysis required 3-D analogy for a true solution, but the 2-D shear deformation theory gives an unrealistic solution.
iv. The 3-D exact plate model developed in this study is variationally consistent and can be used in the analysis of any category of the plate.

Nomenclature

CPT Classical plate theory
RPT Refined plate theories
FSDT First order shear deformation plate theory
TSDT Trigonometric shear deformation theory
ESDT Exponential shear deformation theory
PSDT Polynomial shear deformation theory
HSDT Higher order shear deformation plate theories
CCCC Clamped supported at all the edges.
SSSS Simply supported at all the edges.
CSCS Clamped at two adjacent edges and the other simply supported
CCFS Clamped at the first and second edges and the other edges, free and simply supported respectively.
w Deflection
u In-plane displacement along x-axis
v In-plane displacement along y-axis
θ_{sx} Shear deformation rotation along x axis
θ_{sy} Shear deformation rotation along the y axis
ε_x Normal strain along x axis
ε_y Normal strain along y axis
ε_z Normal strain along z axis
γ_{xy} Shear strain in the plane parallel to the x-y plane
γ_{xz} Shear strain in the plane parallel to the x-z plane
γ_{yz} Shear strain in the plane parallel to the y-z plane
x Horizontal co-ordinate
y Diagonal co-ordinate
z Vertical co-ordinate
a Spatial dimensions of the plate along x -axes
b Spatial dimensions of the plate along y-axes
t Spatial dimensions of the plate along z-axes
R Non-dimensional form of coordinates x-axes
Q Non-dimensional form of coordinates x-axes
S Non-dimensional form of coordinates x-axes
β Aspect ratio (b/a)
μ Poisons ratio
E Modulus of elasticity of the plate
σ_x Stress normal along x axis
σ_y Stress normal along the y axis
σ_z Stress normal along the z axis
τ_{xy} Shear stress along the x-y axis

τ_{xz} Shear stress along the x-z axis

τ_{yz} Shear stress along the y-z axis

D^* Rigidity for three-dimensional thick plate

D Rigidity of the CPT or incomplete three-dimensional thick plate

$\prod$ Total potential energy function

U Algebraic summation of strain energy

V External work for buckling load

h Shape function of the plate

A_1 Coefficient of deflection

A_2 Coefficient of shear deformation along x-axis

A_3 Coefficient of shear deformation along y-axis

q Uniformly distributed load of the plate

$\int_0^1$ Integral operation showing upper and lower limit from 0 to 1

$\iint_0^1$ Double integral operator showing upper and lower limit from 0 to 1

$\iiint$ Triple integral operator showing upper and lower limit from 0 to 1

$k_x = \int_0^1 \int_0^1 \left(\frac{\partial^2 h}{\partial R^2}\right)^2 dRdQ$ Double integral operation with fourth partial derivative of h with respect to R

$k_{xy} = \int_0^1 \int_0^1 \left(\frac{\partial^2 h}{\partial R \partial Q}\right)^2 dRdQ$ Double integral operation with fourthpartial derivative of h with respect to R and Q

$k_y = \int_0^1 \int_0^1 \left(\frac{\partial^2 h}{\partial Q^2}\right)^2 dRdQ$ Double integral operation with fourth partial derivative of h with respect to Q

$k_z = \int_0^1 \int_0^1 \left(\frac{\partial h}{\partial R}\right)^2 dRdQ$ Double integral operation with second partial derivative of h with respect to R

$k_{2z} = \int_0^1 \int_0^1 \left(\frac{\partial h}{\partial Q}\right)^2 dRdQ$ Double integral operation with second partial derivative of h with respect to R

$k_h = \int_0^1 \int_0^1 h \, . dRdQ$ Double integral operation with partial derivative of h with respect to R an Q

References

[1] F. Onyeka, B. O. Mama, C. Nwa-David, Application of variation method in three dimensional stability analysis of rectangular plate using various exact shape functions, *Nigerian Journal of Technology*, Vol. 41, No. 1, pp. 8–20-8–20, 2022.

[2] F. Onyeka, T. Okeke, C. Nwa-David, Static and Buckling Analysis of a Three-Dimensional (3-D) Rectangular Thick Plates Using Exact Polynomial Displacement Function, *European Journal of Engineering and Technology Research*, Vol. 7, No. 2, pp. 29-35, 2022.

[3] C. Nwoji, B. Mama, H. Onah, C. Ike, Kantorovich-vlasov method for simply supported rectangular plates under uniformly distributed transverse loads, *methods*, Vol. 14, No. 15, pp. 16, 2017.

[4] F. Onyeka, F. Okafor, Buckling solution of a three-dimensional clamped rectangular thick plate using direct variational method, *building structure*, Vol. 1, pp. 3, 2021.
[5] K. Chandrashekhara, 2001, *Theory of plates*, Universities press,
[6] F. C. Onyeka, C. D. Nwa-David, T. E. Okeke, Study on Stability Analysis of Rectangular Plates Section Using a Three-Dimensional Plate Theory with Polynomial Function.
[7] F. Onyeka, T. Okeke, Elastic bending analysis exact solution of plate using alternative i refined plate theory, *Nigerian Journal of Technology*, Vol. 40, No. 6, pp. 1018–1029-1018–1029, 2021.
[8] F. Onyeka, Critical lateral load analysis of rectangular plate considering shear deformation effect, *Global Journal of Civil Engineering*, Vol. 1, pp. 16-27, 2020.
[9] J. N. Reddy, 2006, *Theory and analysis of elastic plates and shells*, CRC press,
[10] P. Gujar, K. Ladhane, Bending analysis of simply supported and clamped circular plate, *International Journal of Civil Engineering*, Vol. 2, No. 5, pp. 69-75, 2015.
[11] F. Onyeka, Effect of stress and load distribution analysis on an isotropic rectangular plate, *Arid Zone Journal of Engineering, Technology and Environment*, Vol. 17, No. 1, pp. 9-26, 2021.
[12] F. Onyeka, F. Okafor, H. Onah, Application of a new trigonometric theory in the buckling analysis of three-dimensional thick plate, *International Journal of Emerging Technologies*, Vol. 12, No. 1, pp. 228-240, 2021.
[13] Y. M. Ghugal, P. D. Gajbhiye, Bending analysis of thick isotropic plates by using 5th order shear deformation theory, *Journal of Applied and Computational Mechanics*, Vol. 2, No. 2, pp. 80-95, 2016.
[14] F. Onyeka, D. Osegbowa, Stress analysis of thick rectangular plate using higher order polynomial shear deformation theory, *FUTO Journal Series–FUTOJNLS*, Vol. 6, No. 2, pp. 142-161, 2020.
[15] F. Onyeka, T. Okeke, New refined shear deformation theory effect on non-linear analysis of a thick plate using energy method, *Arid Zone Journal of Engineering, Technology and Environment*, Vol. 17, No. 2, pp. 121-140, 2021.
[16] R. Mindlin, Influence of rotatory inertia and shear on flexural motions of isotropic, elastic plates, 1951.
[17] E. Reissner, The effect of transverse shear deformation on the bending of elastic plates, 1945.
[18] F. C. Onyeka, T. E. Okeke, Analysis of critical imposed load of plate using variational calculus, *Journal of Advances in Science and Engineering*, Vol. 4, No. 1, pp. 13-23, 2021.
[19] J. C. Ezeh, O. M. Ibearugbulem, L. O. Ettu, L. S. Gwarah, I. C. Onyechere, Application of shear deformation theory for analysis of CCCS and SSFS rectangular isotropic thick plates, *Journal of Mechanical and Civil Engineering (IOSR-JMCE)*, Vol. 15, No. 5, pp. 33-42, 2018.
[20] R. Szilard, Theories and applications of plate analysis: classical, numerical and engineering methods, *Appl. Mech. Rev.*, Vol. 57, No. 6, pp. B32-B33, 2004.
[21] B. Mama, C. Nwoji, C. Ike, H. Onah, Analysis of simply supported rectangular Kirchhoff plates by the finite Fourier sine transform method, *International Journal of Advanced Engineering Research and Science*, Vol. 4, No. 3, pp. 237109, 2017.
[22] F. Onyeka, B. Mama, C. Nwa-David, Analytical modelling of a three-dimensional (3D) rectangular plate using the exact solution approach, *IOSR Journal of Mechanical and Civil Engineering*, Vol. 11, No. 1, pp. 10-22, 2022.
[23] S. Timoshenko, S. Woinowsky-Krieger, 1959, *Theory of plates and shells*, McGraw-hill New York,
[24] F. Onyeka, B. Mama, T. Okeke, Exact three-dimensional stability analysis of plate using a direct variational energy method, *Civil Engineering Journal*, Vol. 8, No. 1, pp. 60-80, 2022.
[25] N. Osadebe, C. Ike, H. Onah, C. Nwoji, F. Okafor, Application of the Galerkin-Vlasov method to the Flexural Analysis of simply supported Rectangular Kirchhoff Plates under uniform loads, *Nigerian Journal of Technology*, Vol. 35, No. 4, pp. 732-738, 2016.
[26] C. Nwoji, B. Mama, C. Ike, H. Onah, Galerkin-Vlasov method for the flexural analysis of rectangular Kirchhoff plates with clamped and simply supported edges, *IOSR Journal of Mechanical and Civil Engineering*, Vol. 14, No. 2, pp. 61-74, 2017.
[27] C. Ike, Equilibrium approach in the derivation of differential equations for homogeneous isotropic Mindlin plates, *Nigerian Journal of Technology*, Vol. 36, No. 2, pp. 346-350, 2017.
[28] F. Williams, Structural Stability of Columns and Plates NGR Iyengar Ellis Horwood Limited, Chichester. 1988. 316 pp. Illustrated.£ 22.50, *The Aeronautical Journal*, Vol. 93, No. 923, pp. 111-111, 1989.
[29] C. C. Ike, Fourier series method for finding displacements and stress fields in hyperbolic shear deformable thick beams subjected to distributed transverse loads, *Journal of Computational Applied Mechanics*, Vol. 53, No. 1, pp. 116-131, 2022.
[30] O. M. Ibearugbulem, J. C. Ezeh, L. O. Ettu, L. S. Gwarah, Bending analysis of rectangular thick plate using polynomial shear deformation theory, *IOSR Journal of Engineering (IOSRJEN)*, Vol. 8, No. 9, pp. 53-61, 2018.

[31] F. Onyeka, C. Nwa-David, E. Arinze, Structural imposed load analysis of isotropic rectangular plate carrying a uniformly distributed load using refined shear plate theory, *FUOYE Journal of Engineering and Technology,* Vol. 6, No. 4, pp. 414-419, 2021.

[32] A. S. Sayyad, Y. M. Ghugal, Bending and free vibration analysis of thick isotropic plates by using exponential shear deformation theory, *Applied and Computational mechanics,* Vol. 6, No. 1, 2012.

[33] F. Onyeka, E. T. Okeke, Analytical solution of thick rectangular plate with clamped and free support boundary condition using polynomial shear deformation theory, *Advances in Science, Technology and Engineering Systems Journal,* Vol. 6, No. 1, pp. 1427-1439, 2021.

[34] J. Mantari, A. Oktem, C. G. Soares, A new trigonometric shear deformation theory for isotropic, laminated composite and sandwich plates, *International Journal of Solids and Structures,* Vol. 49, No. 1, pp. 43-53, 2012.

[35] F. Onyeka, F. Okafor, H. Onah, Application of exact solution approach in the analysis of thick rectangular plate, *International Journal of Applied Engineering Research,* Vol. 14, No. 8, pp. 2043-2057, 2019.

[36] A. Y. Grigorenko, A. Bergulev, S. Yaremchenko, Numerical solution of bending problems for rectangular plates, *International Applied Mechanics,* Vol. 49, No. 1, pp. 81-94, 2013.

[37] O. M. Ibearugbulem, U. C. Onwuegbuchulem, C. Ibearugbulem, Analytical Three-Dimensional Bending Analyses of Simply Supported Thick Rectangular Plate, *International Journal of Engineering Advanced Research,* Vol. 3, No. 1, pp. 27-45, 2021.

[38] F. Onyeka, B. Mama, Analytical study of bending characteristics of an elastic rectangular plate using direct variational energy approach with trigonometric function, *Emerging Science Journal,* Vol. 5, No. 6, pp. 916-926, 2021.

[39] A. Hadi, A. Rastgoo, A. Daneshmehr, F. Ehsani, Stress and strain analysis of functionally graded rectangular plate with exponentially varying properties, *Indian Journal of Materials Science,* Vol. 2013, 2013.

[40] M. Mousavi Khoram, M. Hosseini, M. Shishesaz, A concise review of nano-plates, *Journal of Computational Applied Mechanics,* Vol. 50, No. 2, pp. 420-429, 2019.

[41] R. Noroozi, A. Barati, A. Kazemi, S. Norouzi, A. Hadi, Torsional vibration analysis of bi-directional FG nano-cone with arbitrary cross-section based on nonlocal strain gradient elasticity, *Advances in nano research,* Vol. 8, No. 1, pp. 13-24, 2020.

[42] M. Mohammadi, A. Farajpour, A. Moradi, M. Hosseini, Vibration analysis of the rotating multilayer piezoelectric Timoshenko nanobeam, *Engineering Analysis with Boundary Elements,* Vol. 145, pp. 117-131, 2022/12/01/, 2022.

[43] M. Z. Nejad, A. Rastgoo, A. Hadi, Exact elasto-plastic analysis of rotating disks made of functionally graded materials, *International Journal of Engineering Science,* Vol. 85, pp. 47-57, 2014.

[44] M. Z. Nejad, A. Hadi, A. Rastgoo, Buckling analysis of arbitrary two-directional functionally graded Euler–Bernoulli nano-beams based on nonlocal elasticity theory, *International Journal of Engineering Science,* Vol. 103, pp. 1-10, 2016.

[45] M. Z. Nejad, A. Hadi, A. Farajpour, Consistent couple-stress theory for free vibration analysis of Euler-Bernoulli nano-beams made of arbitrary bi-directional functionally graded materials, *Structural engineering and mechanics: An international journal,* Vol. 63, No. 2, pp. 161-169, 2017.

[46] M. Z. Nejad, N. Alamzadeh, A. Hadi, Thermoelastoplastic analysis of FGM rotating thick cylindrical pressure vessels in linear elastic-fully plastic condition, *Composites Part B: Engineering,* Vol. 154, pp. 410-422, 2018.

[47] M. Z. Nejad, A. Hadi, A. Omidvari, A. Rastgoo, Bending analysis of bi-directional functionally graded Euler-Bernoulli nano-beams using integral form of Eringen's non-local elasticity theory, *Structural engineering and mechanics: An international journal,* Vol. 67, No. 4, pp. 417-425, 2018.

[48] M. Hosseini, M. Shishesaz, K. N. Tahan, A. Hadi, Stress analysis of rotating nano-disks of variable thickness made of functionally graded materials, *International Journal of Engineering Science,* Vol. 109, pp. 29-53, 2016.

[49] M. Hosseini, M. Shishesaz, A. Hadi, Thermoelastic analysis of rotating functionally graded micro/nanodisks of variable thickness, *Thin-Walled Structures,* Vol. 134, pp. 508-523, 2019.

[50] M. Mohammadi, M. Ghayour, A. Farajpour, Analysis of Free Vibration Sector Plate Based on Elastic Medium by using New Version of Differential Quadrature Method, *Journal of Simulation and Analysis of Novel Technologies in Mechanical Engineering,* Vol. 3, No. 2, pp. 47-56, 2010.

[51] N. GHAYOUR, A. SEDAGHAT, M. MOHAMMADI, WAVE PROPAGATION APPROACH TO FLUID FILLED SUBMERGED VISCO-ELASTIC FINITE CYLINDRICAL SHELLS, *JOURNAL OF AEROSPACE SCIENCE AND TECHNOLOGY (JAST),* Vol. 8, No. 1, pp. -, 2011.

[52] H. Moosavi, M. Mohammadi, A. Farajpour, S. H. Shahidi, Vibration analysis of nanorings using nonlocal continuum mechanics and shear deformable ring theory, *Physica E: Low-dimensional Systems and Nanostructures,* Vol. 44, No. 1, pp. 135-140, 2011/10/01/, 2011.

[53] A. Farajpour, M. Danesh, M. Mohammadi, Buckling analysis of variable thickness nanoplates using nonlocal continuum mechanics, *Physica E: Low-dimensional Systems and Nanostructures,* Vol. 44, No. 3, pp. 719-727, 2011.

[54] A. Farajpour, M. Mohammadi, A. Shahidi, M. Mahzoon, Axisymmetric buckling of the circular graphene sheets with the nonlocal continuum plate model, *Physica E: Low-dimensional Systems and Nanostructures,* Vol. 43, No. 10, pp. 1820-1825, 2011.

[55] M. Danesh, A. Farajpour, M. Mohammadi, Axial vibration analysis of a tapered nanorod based on nonlocal elasticity theory and differential quadrature method, *Mechanics Research Communications,* Vol. 39, No. 1, pp. 23-27, 2012.

[56] A. Farajpour, A. Shahidi, M. Mohammadi, M. Mahzoon, Buckling of orthotropic micro/nanoscale plates under linearly varying in-plane load via nonlocal continuum mechanics, *Composite Structures,* Vol. 94, No. 5, pp. 1605-1615, 2012.

[57] M. Mohammadi, M. Goodarzi, M. Ghayour, S. Alivand, Small scale effect on the vibration of orthotropic plates embedded in an elastic medium and under biaxial in-plane pre-load via nonlocal elasticity theory, 2012.

[58] M. Mohammadi, A. Farajpour, M. Goodarzi, H. Mohammadi, Temperature Effect on Vibration Analysis of Annular Graphene Sheet Embedded on Visco-Pasternak Foundati, *Journal of Solid Mechanics,* Vol. 5, No. 3, pp. 305-323, 2013.

[59] M. Mohammadi, A. Farajpour, M. Goodarzi, R. Heydarshenas, Levy Type Solution for Nonlocal Thermo-Mechanical Vibration of Orthotropic Mono-Layer Graphene Sheet Embedded in an Elastic Medium, *Journal of Solid Mechanics,* Vol. 5, No. 2, pp. 116-132, 2013.

[60] M. Mohammadi, M. Goodarzi, M. Ghayour, A. Farajpour, Influence of in-plane pre-load on the vibration frequency of circular graphene sheet via nonlocal continuum theory, *Composites Part B: Engineering,* Vol. 51, pp. 121-129, 2013.

[61] M. Mohammadi, M. Ghayour, A. Farajpour, Free transverse vibration analysis of circular and annular graphene sheets with various boundary conditions using the nonlocal continuum plate model, *Composites Part B: Engineering,* Vol. 45, No. 1, pp. 32-42, 2013.

[62] M. Mohammadi, A. Farajpour, M. Goodarzi, H. Shehni nezhad pour, Numerical study of the effect of shear in-plane load on the vibration analysis of graphene sheet embedded in an elastic medium, *Computational Materials Science,* Vol. 82, pp. 510-520, 2014/02/01/, 2014.

[63] A. Farajpour, A. Rastgoo, M. Mohammadi, Surface effects on the mechanical characteristics of microtubule networks in living cells, *Mechanics Research Communications,* Vol. 57, pp. 18-26, 2014/04/01/, 2014.

[64] S. Asemi, A. Farajpour, H. Asemi, M. Mohammadi, Influence of initial stress on the vibration of double-piezoelectric-nanoplate systems with various boundary conditions using DQM, *Physica E: Low-dimensional Systems and Nanostructures,* Vol. 63, pp. 169-179, 2014.

[65] S. Asemi, A. Farajpour, M. Mohammadi, Nonlinear vibration analysis of piezoelectric nanoelectromechanical resonators based on nonlocal elasticity theory, *Composite Structures,* Vol. 116, pp. 703-712, 2014.

[66] M. Mohammadi, A. Farajpour, A. Moradi, M. Ghayour, Shear buckling of orthotropic rectangular graphene sheet embedded in an elastic medium in thermal environment, *Composites Part B: Engineering,* Vol. 56, pp. 629-637, 2014.

[67] S. R. Asemi, M. Mohammadi, A. Farajpour, A study on the nonlinear stability of orthotropic single-layered graphene sheet based on nonlocal elasticity theory, *Latin American Journal of Solids and Structures,* Vol. 11, No. 9, pp. 1515-1540, 2014.

[68] M. Mohammadi, A. Farajpour, M. Goodarzi, F. Dinari, Thermo-mechanical vibration analysis of annular and circular graphene sheet embedded in an elastic medium, *Latin American Journal of Solids and Structures,* Vol. 11, pp. 659-682, 2014.

[69] M. Mohammadi, A. Moradi, M. Ghayour, A. Farajpour, Exact solution for thermo-mechanical vibration of orthotropic mono-layer graphene sheet embedded in an elastic medium, *Latin American Journal of Solids and Structures,* Vol. 11, No. 3, pp. 437-458, 2014.

[70] M. Safarabadi, M. Mohammadi, A. Farajpour, M. Goodarzi, Effect of surface energy on the vibration analysis of rotating nanobeam, 2015.

[71] H. Asemi, S. Asemi, A. Farajpour, M. Mohammadi, Nanoscale mass detection based on vibrating piezoelectric ultrathin films under thermo-electro-mechanical loads, *Physica E: Low-dimensional Systems and Nanostructures*, Vol. 68, pp. 112-122, 2015.

[72] M. Goodarzi, M. Mohammadi, M. Khooran, F. Saadi, Thermo-Mechanical Vibration Analysis of FG Circular and Annular Nanoplate Based on the Visco-Pasternak Foundation, *Journal of Solid Mechanics*, Vol. 8, No. 4, pp. 788-805, 2016.

[73] M. Baghani, M. Mohammadi, A. Farajpour, Dynamic and Stability Analysis of the Rotating Nanobeam in a Nonuniform Magnetic Field Considering the Surface Energy, *International Journal of Applied Mechanics*, Vol. 08, No. 04, pp. 1650048, 2016.

[74] M. R. Farajpour, A. Rastgoo, A. Farajpour, M. Mohammadi, Vibration of piezoelectric nanofilm-based electromechanical sensors via higher-order non-local strain gradient theory, *Micro & Nano Letters*, Vol. 11, No. 6, pp. 302-307, 2016.

[75] A. Farajpour, M. Yazdi, A. Rastgoo, M. Mohammadi, A higher-order nonlocal strain gradient plate model for buckling of orthotropic nanoplates in thermal environment, *Acta Mechanica*, Vol. 227, No. 7, pp. 1849-1867, 2016.

[76] A. Farajpour, M. H. Yazdi, A. Rastgoo, M. Loghmani, M. Mohammadi, Nonlocal nonlinear plate model for large amplitude vibration of magneto-electro-elastic nanoplates, *Composite Structures*, Vol. 140, pp. 323-336, 2016.

[77] M. Mohammadi, M. Safarabadi, A. Rastgoo, A. Farajpour, Hygro-mechanical vibration analysis of a rotating viscoelastic nanobeam embedded in a visco-Pasternak elastic medium and in a nonlinear thermal environment, *Acta Mechanica*, Vol. 227, No. 8, pp. 2207-2232, 2016.

[78] A. Farajpour, A. Rastgoo, M. Mohammadi, Vibration, buckling and smart control of microtubules using piezoelectric nanoshells under electric voltage in thermal environment, *Physica B: Condensed Matter*, Vol. 509, pp. 100-114, 2017.

[79] M. Mohammadi, M. Hosseini, M. Shishesaz, A. Hadi, A. Rastgoo, Primary and secondary resonance analysis of porous functionally graded nanobeam resting on a nonlinear foundation subjected to mechanical and electrical loads, *European Journal of Mechanics - A/Solids*, Vol. 77, pp. 103793, 2019/09/01/, 2019.

[80] M. Mohammadi, A. Rastgoo, Nonlinear vibration analysis of the viscoelastic composite nanoplate with three directionally imperfect porous FG core, *Structural Engineering and Mechanics, An Int'l Journal*, Vol. 69, No. 2, pp. 131-143, 2019.

[81] M. Mohammadi, A. Rastgoo, Primary and secondary resonance analysis of FG/lipid nanoplate with considering porosity distribution based on a nonlinear elastic medium, *Mechanics of Advanced Materials and Structures*, Vol. 27, No. 20, pp. 1709-1730, 2020/10/15, 2020.

[82] M. Goodarzi, M. Mohammadi, A. Farajpour, M. Khooran, Investigation of the effect of pre-stressed on vibration frequency of rectangular nanoplate based on a visco-Pasternak foundation, 2014.

[83] A. Hadi, M. Z. Nejad, M. Hosseini, Vibrations of three-dimensionally graded nanobeams, *International Journal of Engineering Science*, Vol. 128, pp. 12-23, 2018.

[84] M. Shishesaz, M. Hosseini, Mechanical behavior of functionally graded nano-cylinders under radial pressure based on strain gradient theory, *Journal of Mechanics*, Vol. 35, No. 4, pp. 441-454, 2019.

[85] M. Shishesaz, M. Hosseini, K. Naderan Tahan, A. Hadi, Analysis of functionally graded nanodisks under thermoelastic loading based on the strain gradient theory, *Acta Mechanica*, Vol. 228, No. 12, pp. 4141-4168, 2017.

[86] Z. Mazarei, M. Z. Nejad, A. Hadi, Thermo-elasto-plastic analysis of thick-walled spherical pressure vessels made of functionally graded materials, *International Journal of Applied Mechanics*, Vol. 8, No. 04, pp. 1650054, 2016.

[87] A. Hadi, M. Z. Nejad, A. Rastgoo, M. Hosseini, Buckling analysis of FGM Euler-Bernoulli nano-beams with 3D-varying properties based on consistent couple-stress theory, *Steel and Composite Structures, An International Journal*, Vol. 26, No. 6, pp. 663-672, 2018.

[88] H. Haghshenas Gorgani, M. Mahdavi Adeli, M. Hosseini, Pull-in behavior of functionally graded micro/nano-beams for MEMS and NEMS switches, *Microsystem Technologies*, Vol. 25, No. 8, pp. 3165-3173, 2019.

[89] A. Barati, M. M. Adeli, A. Hadi, Static torsion of bi-directional functionally graded microtube based on the couple stress theory under magnetic field, *International Journal of Applied Mechanics*, Vol. 12, No. 02, pp. 2050021, 2020.

[90] C. Wang, J. N. Reddy, K. Lee, 2000, *Shear deformable beams and plates: Relationships with classical solutions*, Elsevier,

[91] J. Reddy, A refined nonlinear theory of plates with transverse shear deformation, *International Journal of solids and structures*, Vol. 20, No. 9-10, pp. 881-896, 1984.

[92] J. Xiao, R. Batra, D. Gilhooley, J. Gillespie Jr, M. McCarthy, Analysis of thick plates by using a higher-order shear and normal deformable plate theory and MLPG method with radial basis functions, *Computer Methods in Applied Mechanics and Engineering*, Vol. 196, No. 4-6, pp. 979-987, 2007.

[93] T. Kant, E. Hinton, Numerical analysis of rectangular Mindlin plates by the segmentation method, *Civil Engineering Department, Report: C*, Vol. 365, 1980.

[94] K. Lee, G. Lim, C. Wang, Thick Lévy plates re-visited, *International Journal of Solids and Structures*, Vol. 39, No. 1, pp. 127-144, 2002.